

SOLAR ROAD OPERATING EFFICIENCY AND ENERGY YIELD – AN INTEGRATED APPROACH TOWARDS INDUCTIVE POWER TRANSFER

Aditya Shekhar^{#1}, Stan Klerks^{*2}, Pavol Bauer^{#3}, Venugopal Prasanth^{#4}

^{*}TNO, The Netherlands, ²stan.klerks@tno.nl

[#]Delft University of Technology, ³p.bauer@tudelft.nl

ABSTRACT— One of the first of its kind, a pilot project involving the instalment of solar roads in Krommenie, was successfully implemented by the consortium of the province of North Holland, TNO, Ooms and Imtech. Seen as a living lab for knowledge gathering in this nascent application area, with a potential of widening the proliferation of PV technologies, the testing of the operating performance of the installed solar road stretch is ongoing. In this context, the theoretical model for energy yield of the solar road is developed to facilitate the future comparative analysis with the real-time measured data. A combination of Inductive Power Transfer (IPT) to solar roads has been suggested for convenient charging of e-bikes in stands.

Keywords— energy yield, inductive power transfer (IPT), module, photovoltaic modules, PV, solar, solar roads

1 INTRODUCTION

The development of solar roads to convert insolation on vast stretches of land to electrical energy, otherwise dedicated solely for transportation, is in its nascent stage. A great potential is seen for PV application with the maturing of solar road technology. Apart from increasing the versatility by smart utilization of land resources, widening the cover of renewable energy generation will lead to a sustainable, secure energy future. Efforts in this direction have led to the successful installation of about 70 m of solar road on a bicycle path in Krommenie, the province of North Holland in association with TNO, Ooms and Imtech, shown in Fig. 1.



Fig. 1 Solar road section at Krommenie [1].

The focus of this project is to gain experience on the real world operating characteristics of the solar road with a feasibility report of IPT stationary charging. In this respect, a variety of measurements will be made to gather information on the insolation, operating temperature and energy yield. Initially, a power output of more than 80 Wp/m² was measured under standardized test conditions. This paper develops theoretical models for insolation at the installation site, operating temperature and efficiency and the dc energy yield of the solar road section. These estimations will be used for comparative analysis with the actual measured data to be further used for analysis.

Section 2 discusses the computational results for the solar irradiance received by a horizontal earth surface in the province of North Holland based on the solar hourly position in the year 2015.

In Section 3, the temperature and insolation dependant operating efficiency computation is described and the corresponding d.c power output and annual energy yield per square meter of the road is calculated.

In Section 4, a feasibility analysis for solar e-bike charging based on stationary IPT charging is conducted. Also, for variations in annual yield of solar roads the number of e-bikes is estimated. Section 5 presents the challenges in integration of the two technologies. Finally, Section 6 presents the conclusions.

2 INSOLATION AT 52.494° N, 4.7666° E

In this section, the incident solar irradiance [2] on a horizontal surface at the installation site is computed for the year 2015.

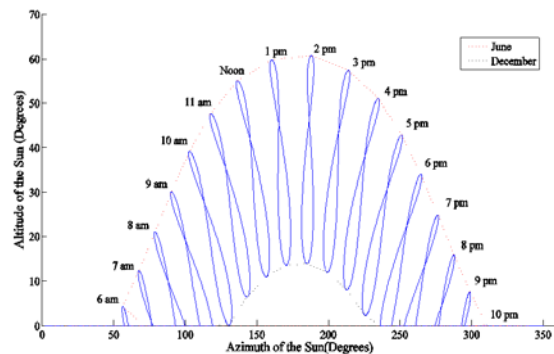


Fig. 2. Solar analemma at 52.494° N, 4.7666° E.

2.1 Solar Analemma

The sun's position [3] is computed in terms of its altitude and azimuth at 52.494° N, 4.7666° E for each hour of the year 2015. The analemma is depicted in Fig. 2. Note that the daylight saving time scheduled followed at the location is not considered while sketching the analemma.

2.2 Solar Irradiation

Corresponding to the altitude and azimuth of the sun, the irradiance (W/m²) for a horizontal surface at the location is computed [4] for every hour of the year 2015 and is shown in Fig. 3. Day 1 is considered to be 1st January 2015.

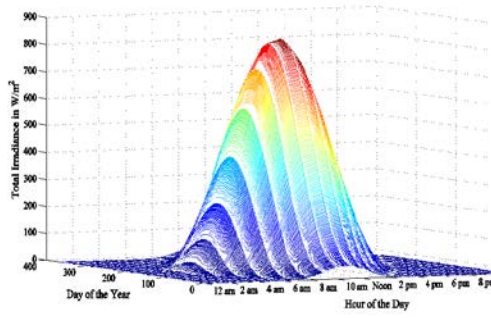


Fig. 3. Irradiance on a horizontal Earth surface at 52.494° N, 4.7666° E.

Both direct and diffuse components of the solar radiation are taken into account. The maximum incident irradiance is 851 W/m². The integral of this over the entire year gives the insolation of 1012 kWh/m² and an average sun hours of 2.77 per day.

3 D.C POWER OUTPUT OF SOLAR ROAD

In this section the operating temperature of the solar road is computed and corresponding efficiency of the module is described for each hour of the year 2015. Based on the specifications of the module, the power output and annual d.c energy yield is calculated.

3.1 Module Specifications

Half section of a solar road consists of 2x270 Wp Soltech photovoltaic (PV) modules. The specifications of the half section are listed in Table I.

Table I: Specifications of Half Section of Solar Road

Parameter	Description
Material	Poly-Crystalline Silicon
No. of Strings	Contact Authors
Cells Per String	Contact Authors
Total Cells	Contact Authors
Cell Dimensions	Contact Authors
STC: 1000 W/m², 25 °C, AM 1.5	
Peak Power (Pmax)	540 Wp
Voltage at Pmax (Vmpp)	Contact Authors
Current at Pmax (Impp)	Contact Authors
Open Circuit Voltage (Voc)	Contact Authors
Short Circuit Current (Isc)	Contact Authors
Temperature Coefficients	
Open Circuit Voltage	-0.32 %/°C
Maximum Power	-0.48 %/°C
Short Circuit Current	0.057 %/°C
Half Section Dimensions	Contact Authors
Efficiency of Module	Contact Authors
Efficiency with surface glass Coating	Contact Authors

The rated output of the entire solar road element is hence 1080 Wp.

3.2 Operating Temperature of Solar Road

Operating temperature of the PV module influences its operating efficiency. In order to calculate the operating temperature, the entire solar road element is assumed to have uniform temperature distribution and the energy inflow and outflow is tracked [2],[5],[6].

The operating temperature of the solar road will depend on the following parameters:

- a) Solar Irradiance: Computed for the year 2015 as described in Section II.

Wind & Ambient Temperature: Convection and radiative heat transfer from the solar road element to the surrounding depends on the wind speed and ambient temperature. Averaged data of the last 10 years was obtained from METEONORM database for the location and is shown in Fig. 4. and Fig. 5. respectively.

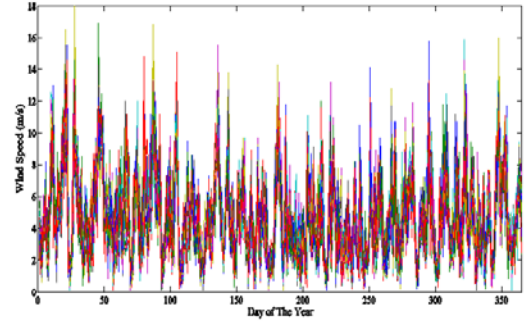


Fig. 4. Hourly wind speed at 52.494° N, 4.7666° E.

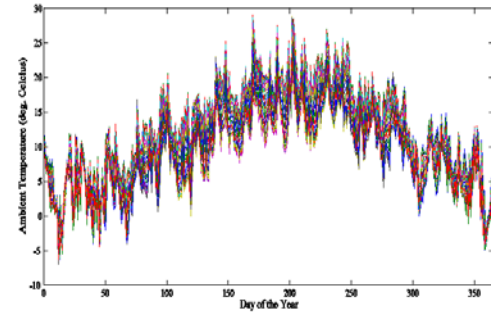


Fig. 5. Hourly ambient temperature at 52.49° N, 4.76° E.

- b) Thermal Coefficients:
 - i) Top surface emissivity is assumed 0.84
 - ii) Bottom Surface emissivity is assumed 0.89
 - iii) Coefficient of Convection: Computed as per [2]
- c) Module Efficiency
- d) Reflectance: assumed 20% (including thick glass surface coating of the solar road).

The required ambient temperature dependant constants like kinematic viscosity of air, air density, air capacity and heat conductivity are considered at the ambient air temperature of 15 °C. The module temperature as per model described in [2],[5] is iteratively computed using (1).

$$T_M = \left(\frac{\phi G_M + h_c T_a + h_{con} T_g}{h_c + h_{con} + h_{r,sky} + h_{r,gnd}} \right) + \left(\frac{h_{r,sky} T_{sky} + h_{r,gnd} T_g}{h_c + h_{con} + h_{r,sky} + h_{r,gnd}} \right) \quad (1)$$

Where,

- T_M is the module temperature in °C
 T_a is the ambient temperature in °C
 T_g is the ground temperature taken as 15 °C

T_{sky} is the sky temperature given by $0.0552 \cdot Ta^{3/2}$
 ϕ is the solar road absorption
 G_M is the insolation on the module
 $h_{r,sky}$ is the radiative heat coefficient between the top surface and sky given by $\epsilon_t \sigma (T_M^2 + T_{sky}^2) (T_M + T_{sky})$
 $h_{r,gnd}$ is the radiative heat coefficient between the bottom surface and ground given by $\epsilon_b \sigma (T_M^2 + T_g^2) (T_M + T_g)$
 ϵ_t is the emissivity of top solar road surface
 ϵ_b is the emissivity of bottom solar road surface
 σ is the Stefan-Boltzmann constant
 h_c is the coefficient of convection computed from the normal and wind speed dependant forced convection
 h_{con} thermal conductivity of concrete casing taken as $1.5 \text{ W/m}^2/\text{C}$

The initial module temperature is assumed to be $Ta+7$ and the solution converges to the actual operating module temperature value in 5 iterations. The computed module temperature for each hour of the year 2015 is shown in Fig. 6.

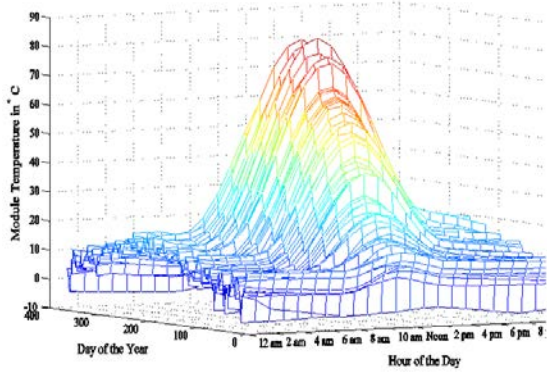


Fig. 6. Estimated Operating Temperature of Solar Road in Year 2015.

The maximum calculated operating temperature is $85.98 \text{ }^\circ\text{C}$. Actual measurements of measurements of temperature are part of the knowledge gathering of the living lab. Based on these measurements the model will be refined.

3.3 Operating Efficiency of Solar Road

The operating efficiency [2] depends on the irradiance and the operating temperature. Greater the irradiance, greater the efficiency while increase in temperature results in lower efficiency. The temperature dependant efficiency is determined from (2) and (3).

$$P_{max}(T_M, G_{stc}) = P_{max,stc} + \frac{dP_{max}}{dT_M} (T_M - T_{stc}) \quad (2)$$

$$\eta(T_M, G_{stc}) = \frac{P_{max}(T_M, G_{stc})}{A_M G_{stc}} \quad (3)$$

Where,

$P_{max}(T_M, G_{stc})$ is the maximum power output of solar road module at operating temperature (T_M) and irradiance (G_{stc}) of 1000 W/m^2 .

$P_{max,stc}$ is the maximum power output in standard test conditions.

$\frac{dP_{max}}{dT_M}$ is the temperature coefficient of the output power.

$\eta(T_M, G_{stc})$ is the temperature dependant module efficiency under standard irradiance

A_M is the area of the solar road module

The irradiance dependence of operating efficiency can be determined from (4)-(7).

$$V_{oc}(T_{stc}, G_M) = V_{oc,stc} \left(\frac{\ln G_M}{\ln G_{stc}} \right) \quad (4)$$

$$I_{sc}(T_{stc}, G_M) = I_{sc,stc} \left(\frac{G_M}{G_{stc}} \right) \quad (5)$$

$$P_{max}(T_{stc}, G_M) = FF \cdot V_{oc}(T_{stc}, G_M) \cdot I_{sc}(T_{stc}, G_M) \quad (6)$$

$$\eta(T_{stc}, G_M) = \frac{P_{max}(T_{stc}, G_M)}{A_M G_{stc}} \quad (7)$$

Where,

$V_{oc}(T_{stc}, G_M)$ is the open circuit voltage at temperature at standard test conditions (T_{stc}) and actual irradiance (G_M).

$I_{sc}(T_{stc}, G_M)$ is the short circuit current

$P_{max}(T_{stc}, G_M)$ is the maximum power output

FF is the module fill factor

$\eta(T_M, G_{stc})$ is the insolation dependant module efficiency under standard temperature conditions

The cumulative impact [2] of change in temperature and insolation on the module efficiency ($\eta(T_M, G_M)$) can be computed from (8)-(10).

$$\eta(T_M, G_M) = \eta(T_{stc}, G_M) \left(1 + k(T_M - T_{stc}) \right) \quad (8)$$

$$k = \frac{d\eta}{dT_M} \left(\frac{1}{\eta_{stc}} \right) \quad (9)$$

$$\frac{d\eta}{dT_M} = \frac{\eta(T_M, G_{stc}) - \eta_{stc}}{T_M - T_{stc}} \quad (10)$$

The hourly estimated efficiency of the solar road is shown in Fig. 7. The maximum efficiency attained is 9.69 %.

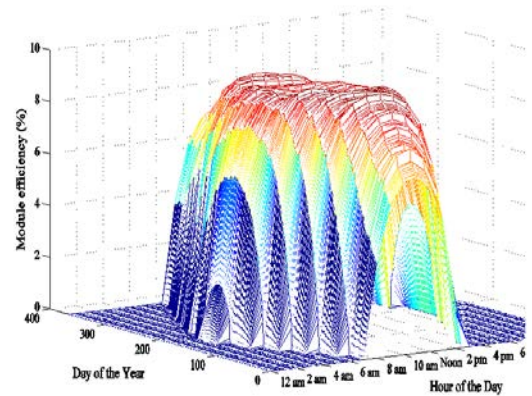


Fig. 7. Estimated Operating Efficiency of the Solar Road in Year 2015.

3.4 D.C Power Output of Solar Road

Together, with information on the hourly computed operating efficiency and the incident radiation, the dc power output of the solar road can be estimated. Fig. 8. shows the estimated dc power output of half a section of the solar road for the year 2015.

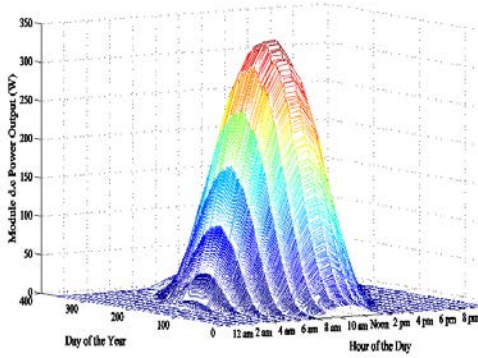


Fig. 8. Estimated dc power output of the solar road in year 2015.

Integrating over the year, the total estimated energy yield is 410 kWh/year per half section of the solar road. With an area of 4.674 m² and the solar irradiation of 4730 kWh/year per half section, the overall annual efficiency is 8.7 %.

The area of entire solar road element is 9.45 m², giving an overall annual efficiency of 8.6 % and a total energy yield of 821 kWh/year, that is, 87 kWh/m²/year. With inverter efficiency of the inverter at 97 %, the solar road is able to inject 84 kWh/m²/year into the grid. In this estimation, the impact of shading, road surface fouling and cloud cover has not been included.

4 INTEGRATING INDUCTIVE POWERING TO SOLAR ROADS

IPT is a process of transferring power through magnetic fields between coils that are displaced by a large air-gap [7], [8]. A complementary development to that of solar roads is that of charging e-bikes by IPT. If L_1 and L_2 are the inductances of the primary and the secondary and M is the mutual inductance then, active power flows through the mutual inductance. However, a large air-gap transformer has large leakage fields ($L_a=L_1-M$, $L_b=L_2-M$) and this increases the circulating reactive power. In order to nullify this effect, capacitors are designed suitably and placed appropriately (series or parallel or a combination) in both the primary and secondary and tuned to resonant frequency. Such a configuration with capacitors in series to both primary and secondary (SS) is shown in Fig. 9. In this figure, the winding resistance are represented as R_1 and R_2 with load resistance as R_L . It has the advantage that the source supplies only the real power while the reactive power circulates between the capacitor and inductor respectively.

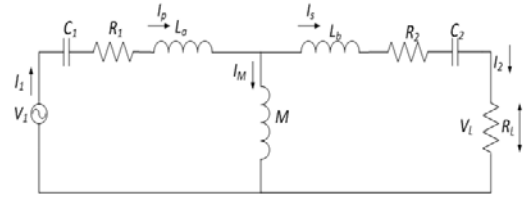


Fig. 9. Modelling the circuit of an IPT system.

When the capacitors are connected in series to both the primary and secondary, the compensation is referred to as SS. In such a case, the output power of an IPT system, P_2 and magnetic primary-secondary efficiency can be quantified in terms of the parameters of the IPT system such as quality factor of the secondary Q_2 and the resonant angular frequency ω_0 as.

$$P_2 = \frac{I_1^2 M^2 Q_2 \omega_0}{L_2} \quad (11)$$

$$\eta = \frac{R_L I_s^2}{R_L I_s^2 + R_2 I_s^2 + R_1 I_p^2} \quad (12)$$

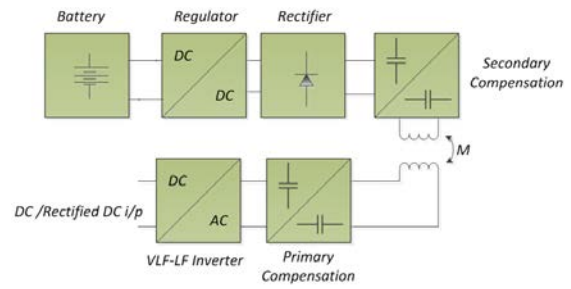


Fig. 10. Basic block diagram of a IPT system.

In the first development, IPT charge pads can be installed at parking lots specifically designed for e-bikes and can be used for charging them when they are parked. This process is referred to as stationary charging. To signify this concept, the following calculations are performed:

- The actual energy yield of a 70m solar road stretch of 120 m² is conservatively estimated as 10,000 kWh/yr. [9].
- The battery capacity of e-bikes in Netherlands can be estimated from a popular manufacturer i.e. Gazelle e-bikes. The battery capacity of one such e-bike is 312 Wh, 8.67 Ah at 36 V [10].
- Assuming overall system efficiency of charging of the bike and IPT system to be 90%, the total number of e-bikes that can be charged is 25675 /yr. This translates to approximately 79 e-bikes/day.

The above calculations signify the immense possibility of stationary charging e-bikes from solar roads. An artistic impression of such an integrated Solar PV for e-bike charging is indicated in Fig. 11.



Fig. 11. Artistic impression of a solar road shed at TU Delft [11].

Solar roads can offer an option of designing similar bike parks with lanes capable of generating energy. Also, a variation in the number of e-bikes charged for varying annual yield of solar roads is presented in Fig. 12. For a yield of 11000 kWh/yr (10% increase), the number of e-bikes increases to 87. This further signifies the potential for integrating the two technologies. A further extension of this step involves powering the bikes as they are moving along the bike lane. Such a concept can yield a bike lane that self-powers and delivers power to the bike as it is moving.

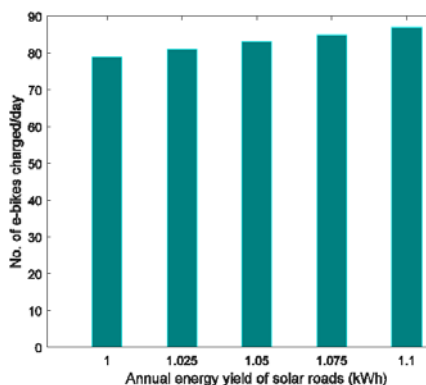


Fig. 12. Number of e-bikes charged for varying annual yield of solar roads.

5 CHALLENGES IN INTEGRATION

A number of challenges have been identified for the integration of IPT and solar roads. Some of these include:

- The sizing, shape and design of the coils that need to be added to both the primary coil and the secondary/pickup attached to the e-bike. Attaching the pickup to the stand is a solution.
- The problems caused due to eddy currents in the solar roads due to the magnetic fields emanating from the primary coils. This leads to heating and hence reduced efficiency of power transfer. A possible solution to this problem is to bypass the solar roads by shaping the fields through ferrites and

placing them in between the solar road sections.

6 CONCLUSION

Based on the latitude and longitude of the province of North Holland, the sun's hourly altitude and azimuth was computed and the corresponding direct and diffuse irradiance on a horizontal surface was estimated.

Temperature model based on the energy balance principle was used to create estimates on the operating temperature of the solar road. The hourly operating efficiency was computed corresponding to the irradiance and the temperature.

Finally the annual energy yield of the solar road was calculated to be 84 kWh/m²/year with an overall efficiency of 8.6 %.

The first generation solar road technology focuses on safety, structural integrity and robustness of the installation. Ageing and real time operational aspects influence the scalability of the application. Measured data will be used for comparative analysis with the models developed in this paper to identify various opportunities to optimize the system for lowering costs and improving the energy yield.

Finally, a possibility of integrating solar roads with inductive powering for charging e-bikes in parking lots is discussed with charging of up to 79 e-bikes for 10000 kWh/day. Economic viability of charging by inductive power transfer is explored in [12].

ACKNOWLEDGMENTS

The authors would like to thank Prof. Olindo Isabella of the Delft University of Technology for his guidance in developing the computational models, and want to thank the consortium partners of SolaRoad for their continuous support in the development in this nascent application area.

REFERENCES

- [1] [Online]. Available: http://www.solaroad.nl/_beeld-bank [Accessed: 15 02 2015].
- [2] K. Jager, O. Isabella, A. H.M. Smets, R. A.C.M.M. Van Swaaij and M. Zeman, "Solar Energy: Fundamentals, Technology and Systems," 2014, pp. 225-339.
- [3] Astronomical Applications Department of The U.S. Naval Observatory, "The Astronomical Almanac," Approximate Solar Coordinates [Online]. Available: <http://aa.usno.navy.mil/faq/docs/SunApprox.php>
- [4] Rigollier C., Bauer O., Wald L., On the clear sky model of the 4th European Solar Radiation Atlas with respect to the Heliosat method, Solar Energy, 68(1), 33-48, 2000.
- [5] M. K. Fuentes, "A Simplified Thermal Model for Flat-Plate Photovoltaic Arrays," Tech. Rep. (Sandia National Laboratories, 1987).
- [6] A. Jones and C. Underwood, Solar Energy 70, 349 (2001).

- [7] Prasanth, V.; Bauer, P., "Distributed IPT Systems for Dynamic Powering: Misalignment Analysis," *Industrial Electronics, IEEE Transactions on* , vol.61, no.11, pp.6013,6021, Nov. 2014.
- [8] Chopra, S.; Prasanth, V.; Mansouri, B.E.; Bauer, P., "A contactless power transfer — Supercapacitor based system for EV application," *IECON 2012 - 38th Annual Conference on IEEE Industrial Electronics Society* , vol., no., pp.2860,2865, 25-28 Oct. 2012.
- [9] [Online]. Available: <http://www.solaroad.nl/en/> [Accessed: 28 06 2015].
- [10] Royal Dutch Gazelle, *Brochure Electric Bikes* [online]. Available: <http://www.gazellebikes.com/service/brochures>
- [11] Y.Peng, "Design of Photovoltaics e-bikes charging station", TU Delft Institutional Repository, 2014.
- [12] Aditya Shekhar, Mark Bolech, Venugopal Prasanth and Pavol Bauer; "Economic Considerations for On-Road Wireless Charging Systems," *IEEE PELS Workshop on Emerging Technologies Wireless Technology*, Kaist, Korea, WoW, 2015.